



**HAL**  
open science

## Frequency domain adaptative filtering against pulsed interference : performance analysis over Europe

Mathieu Raimondi, Christophe Macabiau, Olivier Julien

► **To cite this version:**

Mathieu Raimondi, Christophe Macabiau, Olivier Julien. Frequency domain adaptative filtering against pulsed interference : performance analysis over Europe. ION NTM 2008, National Technical Meeting of The Institute of Navigation, Jan 2008, San Diego, United States. pp 164-176. hal-01022137

**HAL Id: hal-01022137**

**<https://enac.hal.science/hal-01022137>**

Submitted on 30 Sep 2014

**HAL** is a multi-disciplinary open access archive for the deposit and dissemination of scientific research documents, whether they are published or not. The documents may come from teaching and research institutions in France or abroad, or from public or private research centers.

L'archive ouverte pluridisciplinaire **HAL**, est destinée au dépôt et à la diffusion de documents scientifiques de niveau recherche, publiés ou non, émanant des établissements d'enseignement et de recherche français ou étrangers, des laboratoires publics ou privés.

# Frequency Domain Adaptive Filtering Against Pulsed Interference: Performance Analysis Over Europe

Mathieu RAIMONDI, *ENAC*  
Christophe MACABIAU, *ENAC*  
Olivier JULIEN, *ENAC*

## BIOGRAPHIES

Mathieu RAIMONDI is a signal processing engineer. He graduated in 2005 from the ENAC (Ecole Nationale de l'Aviation Civile) in Toulouse, France. He is now a PhD Student at the ENAC and studies signal processing solutions to fight interference on GNSS receivers.

Christophe MACABIAU graduated as an electronics engineer in 1992 from the ENAC in Toulouse, France. Since 1994, he has been working on the application of satellite navigation techniques to civil aviation. He received his Ph.D. in 1997 and has been in charge of the signal processing lab of the ENAC since 2000.

Olivier Julien is an assistant professor at the ENAC, Toulouse, France. His research interests are GNSS receiver design, GNSS multipath and interference mitigation and GNSS interoperability. He received his engineer degree in 2001 in digital communications from ENAC and his PhD in 2005 from the Department of Geomatics Engineering of the University of Calgary, Canada.

## ABSTRACT

Civil Aviation standardisation bodies (ICAO, RTCA, EUROCAE) are currently investigating the use of Global Navigation Satellite Systems (GNSS) as a stand-alone navigation solution for civil aircraft. For obvious safety reasons, on-board GNSS receivers must guarantee minimum requirements in given phases of flights. These requirements, dependent upon the system and signals used, are stated in the Minimum Operational Performance Specification (MOPS), published (or being published) by the corresponding authorities. With that respect, the future use of Galileo E5 and GPS L5 bands has raised, among others, interference issues. Indeed, pre-existent RF systems emit in this band, though interfering with the E5/L5 signals. The main threat was identified as being DME/TACAN ground beacons pulsed emissions

[RTCA, 2004]. Without any mitigation capability, these systems can disturb the proper functioning of on-board GNSS receivers, preventing them from complying with safety requirements. Two Interference Mitigation Techniques (IMT) have been proposed to fight this threat, the Temporal Blanker (TB) and the Frequency Domain Adaptive Filtering (FDAF). The TB technique [Grabowsky, 2002] offers a fairly simple implementation and was shown [Bastide, 2004] to provide enough benefits to ensure that the specified requirements were met in all phases of flights for a GPS L5 or Galileo E5 receiver. However, it was also demonstrated that the resulting performances were meeting the requirements by only a small margin on the worst locations.

In contrast, the FDAF is a more demanding mitigation technique against pulsed interference in terms of required resources but [Raimondi, 2006] showed that it could bring a stronger margin with respect to the civil aviation requirements. Simulations [Raimondi, 2006] showed that the use of FDAF allowed an decrease of the post-correlation  $C/N_0$  over the worst DME/TACAN interference environment that can be found in Europe, so called the European "hot spot".

However, simulations obtained through running an accurate model of a GNSS receiver are often extremely time-consuming, and, in this condition, it is a cumbersome work to draw a world map checking the good functioning of FDAF in all locations. It is then interesting to find a simplified theoretical way to derive the post-correlation  $C/N_0$  degradation suffered by the signal as a function of the interference environment, using an FDAF technique. The aim of this article is to describe a new simulation tool aiming at calculating this degradation in all location in a very short time. Results are first confirmed and then compared to temporal blanker's one.

## INTRODUCTION

The future use of the Galileo E5 and GPS L5 bands by the civil aviation community raises new issues, notably concerning pulsed interference. These bands suffer concomitantly radio frequency emissions from DME (Distance Measuring Equipment), TACAN (TACTical Air Navigation), JTIDS (Joint Tactical Information Distribution System) and MIDS (Multifunctional Information Distribution System) systems. These interferences, if ignored, significantly disturb GNSS receivers functioning and prevent them from meeting civil aviation requirements. In order to be used onboard civil aircrafts, the GPS L5 and Galileo E5 signals have to be processed so that they allow specified minimum performances.

In the following, the study will focus on the E5a/L5 band, as this band is more impacted by pulsed interference than the E5b one [Bastide, 2004]. Also, it can be shown that the impact of JTIDS/MIDS signals on GPS L5 and Galileo E5a signal processing is very low with respect to DME/TACAN signals'one. Consequently they will be omitted herein for simplification purposes.

The usual figure of merit used to look at the impact of an interference is the degradation of the post-correlation  $C/N_0$ . Indeed, it constitutes a good indicator of acquisition and data demodulation performance, which are critical operations for the receiver.

In order to evaluate the performance of a DME/TACAN mitigation technique, it is necessary to draw a map of the post-correlation  $C/N_0$  degradations suffered by the GNSS receiver over Europe. Given the location of DME/TACAN beacons, the interference scenarios will depend on the user location and has to take into account the emission powers and the carrier frequencies of each visible DME/TACAN ground station. These values are given in [Bastide, 2004] and are used herein. The TB performance assessment can be found in [Bastide, 2004]. It shows that GNSS receivers using the technique would comply with ICAO requirements: using TB, no loss of lock is experienced and the  $C/N_0$  ratio stays above the minimum requirements.

On the other hand, FDAF is proposed as an algorithm that would guarantee higher  $C/N_0$  levels in presence of interference. This has already been shown over the hot spot using simulations, but this result needs to be generalized whatever the user location. Performing this using a simulator would be too heavy and time-consuming, so that this paper proposes a Matlab tool predicting the degradations. It allows, in addition to obtaining results quickly, disposing of a second tool enabling to corroborate the results, to be more confident in them.

The here after paper will therefore describe the interference threats before FDAF. Then, the

strategy adopted to design the Matlab tool is detailed, and finally FDAF performance are analyzed and compared to the Temporal Blankers' ones.

## THREAT DESCRIPTION

The study focuses on the major threat in the L5 band: DME/TACAN ground beacons emissions. Their emissions interfere with the E5a/L5 GNSS signals, and can prevent the GNSS receivers from acquiring and tracking satellites if no care is taken. The quoted beacons emit pulse pairs, each pulse being a Gaussian curve modulated by a cosine [Monnerat, 2003]. It can be modelled as follow:

$$s(t) = \sqrt{P} \times \sum_{k=1}^N \left( e^{-\frac{\alpha(t-t_k)^2}{2}} + e^{-\frac{\alpha(t-\Delta t-t_k)^2}{2}} \right) \times \cos(2\pi f_t t + \theta_t) \quad (1)$$

(1)

Where:

- $P$  is the DME/TACAN peak power at receiver antenna level (W),
- $\{t_k\}$  is the set of pulse pairs arrival times,
- $f_t$  is the frequency of the received DME/TACAN signal (Hz),
- $\theta_t$  is DME/TACAN signal carrier phase at the GNSS receiver antenna port,
- $\Delta t$  is the inter-pulse interval ( $=12\mu\text{s}$ ),
- $\alpha = 4.5 \times 10^{11} \text{ s}^{-2}$ .

Figure 1 represents a DME/TACAN pulse pair. The ground stations emit up to 2700 (DME) / 3600 (TACAN) pulse pairs per second (ppps). The actual ppps values are proper to each station.

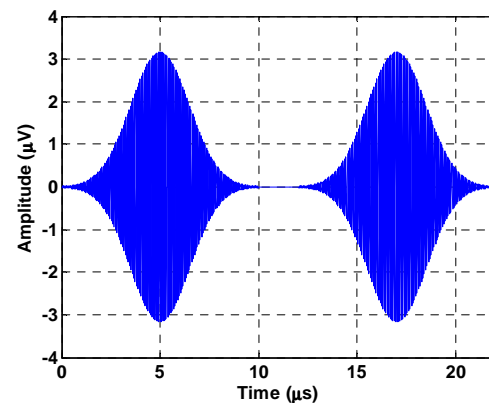


Figure 1: DME signal pattern.

For an onboard GNSS receiver, the operational environment is then composed of a combination of signals emitted by DME/TACAN beacons with

different powers, carrier frequencies and pulse pair repetition rate.

### TEMPORAL BLANKER DESCRIPTION

The temporal blanker, referred as digital pulse blanking in [Grabowsky, 2002], was the first technique proposed to mitigate pulsed interference effects on GNSS receivers. The temporal blanker detects pulsed interference observing the input signal amplitude, and replace the corrupted samples by zero. The post-correlation  $C/N_0$  degradation theoretical derivation used in the following is available in [Bastide, 2004].

### FDAF DESCRIPTION

The FDAF technique is a pulsed interference removal technique working in the frequency domain. It was first proposed as a DME/TACAN mitigation technique in [Monnerat, 2003]. The technique intervenes in the same place as the temporal blanker, after the ADC (Analog to Digital Converter). Therefore the input of the algorithm is a quantized and sampled signal. It performs an estimation of the incoming signal's Fourier transform, by operating a Fast Fourier Transform (FFT) on a pre-defined number of samples ( $R$ ). It then compares the amplitude of each point of the signal's Fourier representation to a certain threshold. Note that since the incoming signal is, without disturbances, dominated by thermal noise, the FFT representation of the incoming signal should ideally be flat (white). This assumption allows the determination of a threshold that would represent the usual noise level, with a certain false alarm rate. If certain points of the incoming signal's Fourier transform exceed this threshold, they are considered corrupted by an interference and set to zero. Finally, the inverse FFT of the manipulated incoming signal is performed so as to obtain the signal back in the time domain to feed the acquisition/tracking modules.

The relative narrow frequency representation of DME/TACAN signals (~1 MHz, see Figure 2) compared to the E5a/L5 GPS and Galileo signals (~20 MHz wide) allows this targeted blanking.

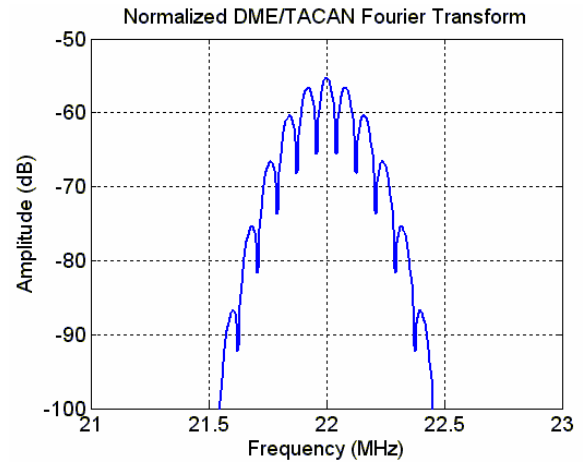


**Figure 2: DME/TACAN Signal Normalized Fourier Transform modulated at 22 MHz**

However, note that this method might not be usable with narrow-band GNSS signals such as CW (Continuous Wave) or NBI (Narrow Band Interference) interference due to its lack of resolution.

In order not to be a computation burden, the Fourier analysis requires the incoming signal to be split into pieces composed of a relatively small pre-determined number of samples. A large number of samples would increase the frequency resolution of the Fourier transform and would likely result into a more relevant blanking technique. However, it will also induce an increase in the computation load (FFT of an increased number of points). A trade-off between performance and computation load has then to be found. In the following tests, this value is set to 128, as [Raimondi, 2006] stated this setting showed good performance and reasonable additional complexity. Indeed, using a sampling frequency of 56 MHz, each window is 2.28  $\mu$ s long, which corresponds to half of the duration of a pulse.

Figure 3 details the functioning of the technique. An example of a piece of signal corrupted by a DME signal is passed through the FDAF.

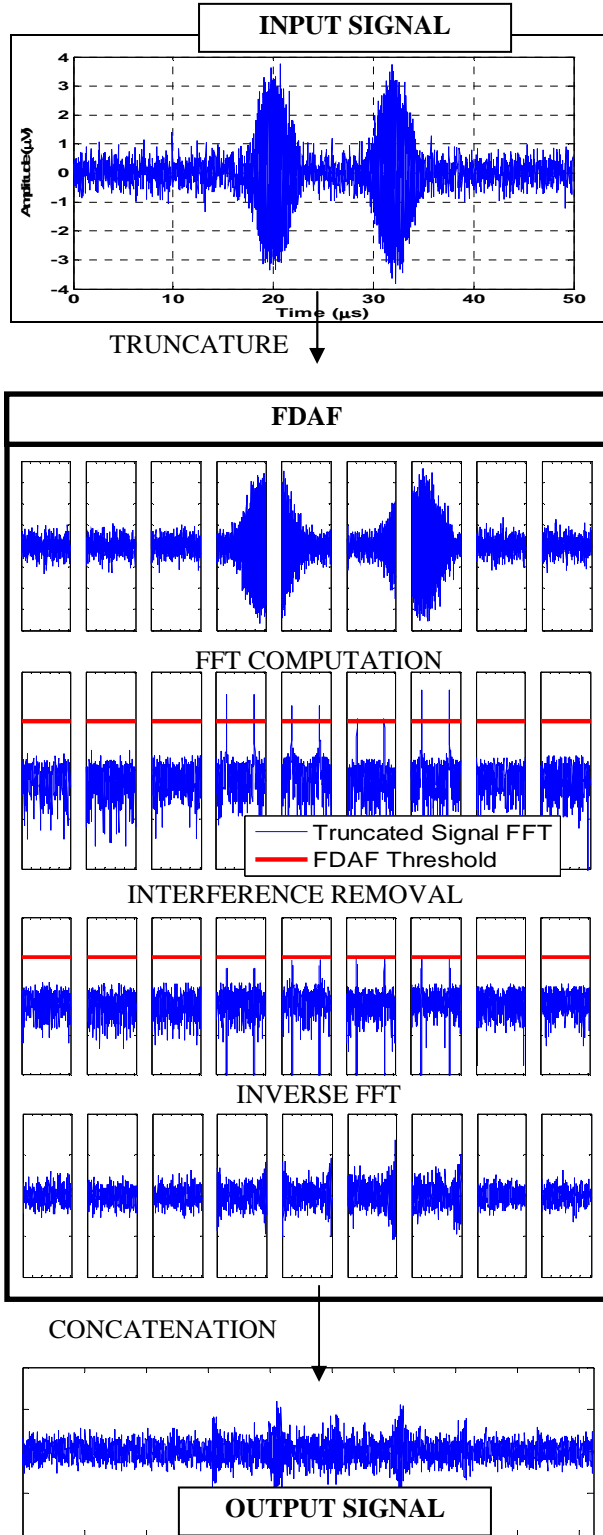


Figure 3: FADF Functioning Scheme.

## SIGNAL ENVIRONMENT ASSUMPTIONS

The GNSS signal is a QPSK modulated L5 code, which reception power equals -155 dBW. The noise is white and Gaussian, and its density equals -200 dBW/Hz. The pulsed interferences follow the theoretical expression given in (1). The visible interferences are determined using the radio electric horizon, and the DME/TACAN signals reception is assumed to follow a Poisson law. Their peak power at receiver front end level is supposed to be attenuated by the DME/TACAN station antenna, propagation and the aircraft antenna.

## C/N<sub>0</sub> DEGRADATION DERIVATION

The presence of interference induces a decrease in the received signal quality. Indeed, the interference can be equivalently modelled as an additive white noise at correlator output [Van Dierendonck, 1996]. Assuming this model is valid in case the interference is processed by one of the proposed IMTs, the carrier to noise ratio at correlator output can be written:

$$\left( \frac{C}{N_0} \right)_{IMT} = \frac{C_{IMT}}{N_{0,IMT} + N_{0,I,IMT}}$$

Where:

- $C$  is the carrier power,
- $N_0$  is the thermal noise density,
- $N_{0,IMT}$  is the thermal noise density if an IMT is applied,
- $C_{IMT}$  is the carrier power if an IMT is applied,
- $N_{0,I,IMT}$  is the equivalent noise density induced by interference, when processed by an IMT.

The applied IMT can be either the TB or the FADF. The theoretical derivation of the post-correlation C/N<sub>0</sub> degradation, in presence of interference and using the TB, is given in [Bastide, 2004]. Here, the IMT considered here is FADF, and the approach used to derive the degradation is the same as the one described in [Bastide, 2004] for the TB: the three components  $C_{IMT}$ ,  $N_{0,IMT}$ , and  $N_{0,I,IMT}$  will be derived independently.

## GNSS CODE POWER LOSS ESTIMATION

FDAF is a filtering process which transfer function is a priori not known, as it is function of the input signal. However, if this equivalent filter could be determined, the useful signal power degradation would be easily computed using the well-known formula:

$$\frac{C_{FDAF}}{C} = \left( \int_{-\infty}^{+\infty} PSD_{GNSS}(f) \times H_{eq,FDAF}(f) df \right)^2 \quad (2)$$

Where:

- $PSD_{GNSS}$  is the base-band normalized PSD of the GNSS code,

Then, the objective of the prediction will be to determine, as a function of the interference environment, the equivalent transfer function of the filter applied by FDAF,  $H_{eq,FDAF}(f)$ .

## THERMAL NOISE LOSS ESTIMATION

Using the same assumption than in the previous paragraph, the degradation suffered by thermal noise is:

$$\frac{N_{0,FDAF}}{N_0} = \int_{-\infty}^{+\infty} PSD_{GNSS}(f) \times |H_{eq,FDAF}(f)|^2 df \quad (3)$$

Here appears the same unknown than in previous section. Determining  $H_{eq,FDAF}(f)$  will allow computing both useful signal and thermal noise degradation.

## INTERFERENCE CONTRIBUTION TO NOISE FLOOR

The contribution of pulsed interference to noise floor has already been studied and derived in [Van Dierendonck, 1996]. In [Bastide, 2004], a derivation of this contribution is proposed, where the TB is used as a mitigation technique. The additive noise density at correlator output is given by:

$$N_{0,I,FDAF} = P_{interf} \times C_{I,FDAF} \quad (4)$$

$$C_{I,FDAF} = \int_{-\infty}^{+\infty} PSD_{I,FDAF} \times PSD_{GNSS} df$$

Where:

- $P_{interf}$  is the interference mean power after front-end filtering,
- $PSD_{I,FDAF}$  is the base-band normalized interference Power Spectral Density,

- $C_{I,FDAF}$  is the interference coefficient, the interference being processed by FDAF.

The interference mean power is determined using an equivalent model, detailed in [Bastide, 2004] where pulses are replaced by equivalent rectangles of duration  $T_{eq}$ . It also uses the statistical characteristics of the signal: the interference arrives to the receiver following a Poisson law of parameter  $\lambda$ , which is directly linked to the PRF. It results in the following expression of  $P_{interf}$ :

$$P_{interf} = P \times (\lambda \times T_{eq}) \times e^{-\lambda \times T_{eq}} \times \left( 1 + (\lambda \times T_{eq}) \times e^{-\lambda \times T_{eq}} \right) \quad (5)$$

Where:

- $T_{eq} = 2.64 \mu s$  is the equivalent duration of a pulse,
- $\lambda$  is the parameter of the Poisson law characterizing the arrival times. In our case, it equals the considered interference PRF.

Therefore, the objective is to estimate the interference coefficient, in case the interference is processed by FDAF.

## PREDICTION TOOL DESCRIPTION

Accordingly with the previous paragraphs, the derivation of the post-correlation  $C/N_0$  degradation for a given interference environment requires the following information:

- The FDAF equivalent transfer function, so as to determine GNSS signal and thermal noise degradation,
- The DME/TACAN PSD after FDAF processing, so as to be able to compute the interference coefficients.

Then, a tool aiming at assessing these variables as a function of the user location has been developed, always keeping in mind to reduce the number of calculations to its minimum. The processing chart is as follows:

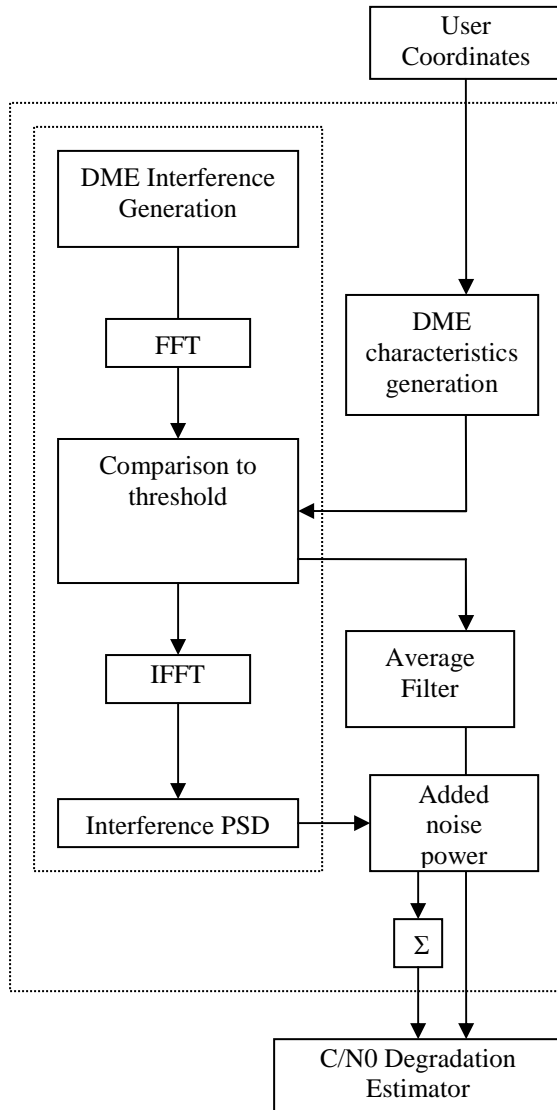


**Figure 4 : Prediction tool Processing Chart.**

The baseline is a database encompassing the following information:

- the coordinates of every ground station emitting DME/TACAN signals in Europe,
- their carrier frequency,
- their Pulse Repetition Frequency.

The coordinates of the user are entered in the DME characteristics generator, which outputs a list of visible DME/TACAN stations and their characteristics: PRF, carrier frequency, and peak power at front-end input.

A map representing all the DME/TACAN ground beacons listed in Europe is shown in Figure 5. It shows that the critical points are mostly located in Western Europe and Turkey.

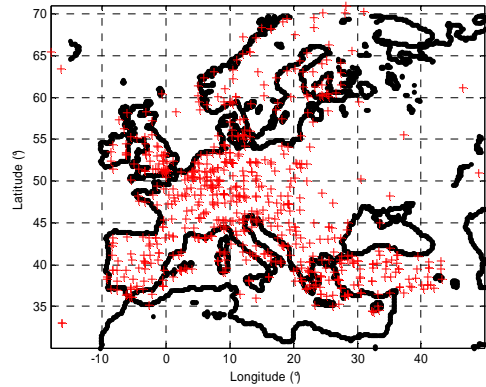


**Figure 5 : European DME/TACAN ground stations.**

The peak power at front-end input is calculated applying the following gains:

- ground station antenna gain,
- free space loss,
- aircraft antenna gain.

The antenna gain pattern used for DME/TACAN station is given in Figure 6. This pattern has been derived from typical DME/TACAN beacons antenna gain patterns [Bastide, 2004].

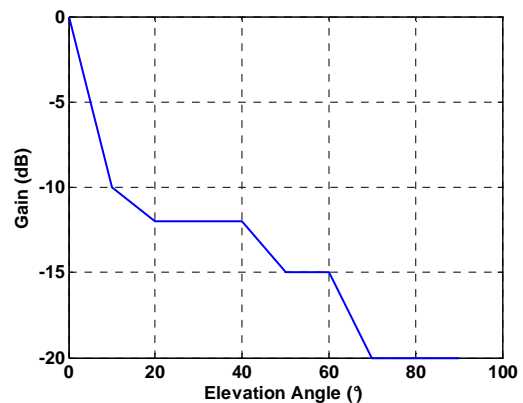


**Figure 6: DME/TACAN antenna gain pattern.**

The free space loss is calculated using the Friis formula, where the loss is a function of the signal carrier frequency and the travelled distance.

The aircraft antenna gain equals -2 dB for all elevations; this value is extracted from the appendix C of [EUROCAE WG-62, 2006]. This antenna gain corresponds to the maximum specified gain at 0° elevation, thus representing the worst case for interference considerations. The results previously published about pulsed interference induced degradation did not take into account this recent and pessimistic assumption. Therefore, the results obtained in this study can not be compared to ancient ones.

This list is then used to generate a DME/TACAN signal as shown in Figure 7. A pulse lasting approximately 20  $\mu\text{s}$ , and taking a margin of 5  $\mu\text{s}$  before the beginning and after the end of it, the signal is generated during 34  $\mu\text{s}$ . It is reminded that only DME signal is generated (no noise, no GNSS signal), as the other signals are assumed to have negligible impact on FDAF functioning assuming the ADC works properly and the FDAF threshold is well chosen.

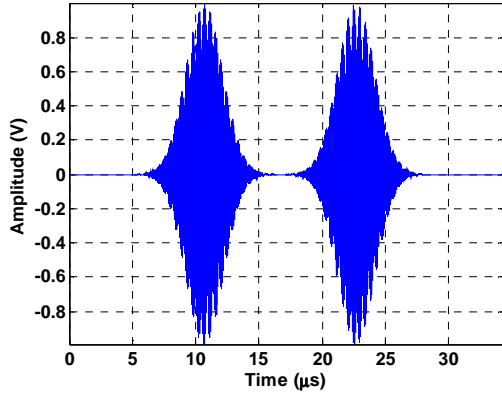


Figure 7: Amplitude 1 DME Pulse Pair.

Then, the signal is sliced in pieces of 128 samples, and the Fast Fourier Transform of each slice is computed (see Figure 8, all the FFTs are superimposed for the plot).

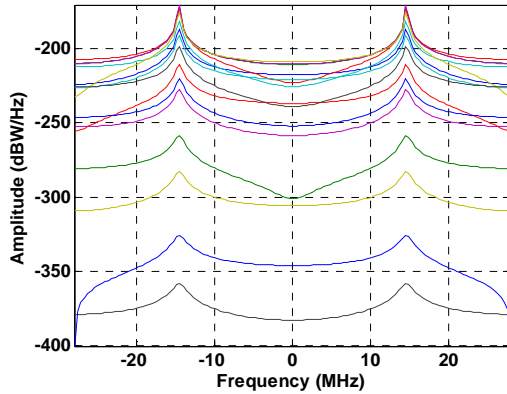


Figure 8: DME signal's FFTs by slice.

An  $N_{win}$  (number of slices contained in 34  $\mu\text{s}$ ) by 128 matrix is now built. The columns stand for frequency bins and the lines for time slots (slice number).

Then, the normalized signal is multiplied by its amplitude given by the DME characteristics generator and compared to the FDAF threshold as follows:

$$FDAF_m(k, f, i) = 1 \text{ if } |FFT(signal)|^2 < \text{Threshold} \quad (6)$$

$$= 0 \text{ if } |FFT(signal)|^2 > \text{Threshold}$$

Where:

- $k$  is the window index,
- $f$  is the frequency,
- $i$  is the ground station index.

The output is an  $N_{win}$  by 128 matrix filled with zeros (if the threshold is exceeded) and ones (if the threshold is not exceeded). This matrix is stored in  $FDAF_m(k, f, i)$ . The process is illustrated in Figure 9, where the input signal is the example shown in Figure 8.

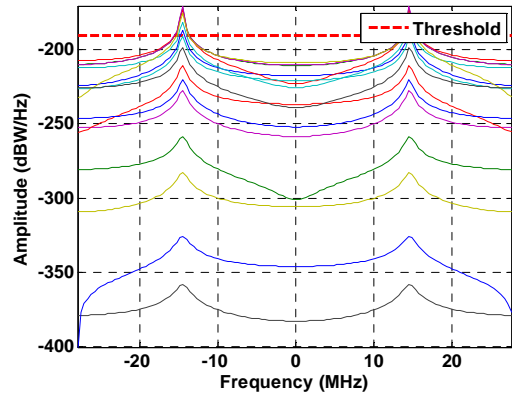


Figure 9 : Comparison of signal FFTs to FDAF threshold.

The DME signal processed by FDAF can now be rebuilt in time domain and the PSD of the obtained signal is estimated through the periodogram formula:

$$PSD_{I,FDAF} = \frac{|FFT(Int_{FDAF})|^2}{R \times N_{win}}$$

Where:

- $Int_{FDAF}$  is the  $R \times N_{win}$  interference signal after being processed by FDAF.

This PSD is then normalized with respect to the PSD of the initial interference (not processed by FDAF), so as to be able to calculate the interference coefficient presented in equation (4).

$$PSD_{I,FDAF} = \frac{PSD_{I,FDAF}}{|PSD_I|}$$

According to equation (4), this interference coefficient shall be multiplied by the mean power



of the DME/TACAN signal at correlator input, which expression is given in equation (5).

The obtained power represents the contribution of one specific DME/TACAN emitter to the noise floor. The total contribution is then the sum of this result applied to each DME/TACAN visible emitter.

$$N_{0,I,FDAF} = \sum_{i=1}^{N_{beacon}} P_{interf,i} \times C_{I,FDAF,i} \quad (7)$$

This result assumes the independence of the interference sources and the absence of collisions. The effect of collisions will be taken into account later on.

The interference contribution to noise floor is now known. The calculation of the two other components of the degradation is detailed in the following section.

### FDAF EQUIVALENT FILTER

As previously seen, one of the objectives is to find the equivalent transfer function representing the processing due to successive FDAF filters.

If the noise and GNSS signals PSD after FDAF processing can be expressed as a function of the same signals' PSD before FDAF processing, the transfer function will be deducible from Wiener-Lee relationships. The periodogram of these signals at FDAF output are:

$$P\hat{S}D(noise_{FDAF}) = \frac{|FFT_{noise,FDAF}(k,f)|^2}{T}$$

$$P\hat{S}D(GNSS_{FDAF}) = \frac{|FFT_{GNSS,FDAF}(k,f)|^2}{T}$$

Where:

- $P\hat{S}D(noise_{FDAF})$  is the PSD estimate of thermal noise, using the periodogram,
- $P\hat{S}D(GNSS_{FDAF})$  is the PSD estimate of the GNSS signal, using the periodogram,
- $FFT_{noise,FDAF}(k,f)$  is the Fast Fourier Transform of the thermal noise, calculated after FDAF processing, computed using the  $k^{\text{th}}$  slice of signal (window),
- $FFT_{GNSS,FDAF}(k,f)$  is the Fast Fourier Transform of the GNSS signal, calculated after FDAF processing, computed using the  $k^{\text{th}}$  slice of signal (window),
- $T$  is the window duration in seconds.

The periodogram being a non-biased estimator, its expectation equals the estimated PSD:

$$E[P\hat{S}D(noise_{FDAF})] = PSD(noise_{FDAF})$$

$$E[P\hat{S}D(GNSS_{FDAF})] = PSD(GNSS_{FDAF})$$

Then, using the FFT linearity, for both noise and GNSS signals:

$$|FFT_{FDAF}(k,f)|^2 = |FFT(k,f)|^2 \times |FDAF(k,f)|^2$$

In this section, the FDAF filters are considered as random variables, which depend upon the received interference. The interference on one side, and the thermal noise and GNSS signals on the other side being independent, thus one can write:

$$E\left[\frac{|FFT(k,f)|^2}{T} \times |FDAF(k,f)|^2\right]$$

$$= E\left[\frac{|FFT(k,f)|^2}{T}\right] \times E\left[|FDAF(k,f)|^2\right]$$

The first term is the expectation of the signals periodogram estimated before FDAF processing. The periodogram being a non-biased PSD estimator:

$$PSD(noise_{FDAF}) = PSD(noise) \times E\left[|FDAF(k,f)|^2\right]$$

$$PSD(GNSS_{FDAF}) = PSD(GNSS) \times E\left[|FDAF(k,f)|^2\right]$$

So the squared module of the FDAF equivalent transfer function is the expectation of the squared FDAF filters, observed on one window  $k$ . For both GNSS signal and thermal noise, the equivalent filter transfer function is:

$$|H_{eq,FDAF}(f)|^2 = E\left[|FDAF(k,f)|^2\right]$$

### FDAF EXPECTATION CALCULATION

The interference reception process being ergodic, the expectation can be written:

$$E\left[|FDAF(k,f)|^2\right] = \lim_{N \rightarrow \infty} \frac{\sum_{k=1}^N |FDAF(k,f)|^2}{N}$$

The expectation is calculated over time, not over experiments. FDAF filters are composed of R values, each value representing one frequency slot, which equal zero or one. Then, the expectation is:

$$\begin{aligned} E\left[FDAF(k, f)\right]^2 &= \lim_{N \rightarrow +\infty} \frac{N^1(f, N)}{N} \\ &= \lim_{N \rightarrow +\infty} \frac{N - N^0(f, N)}{N} \\ &= \lim_{N \rightarrow +\infty} 1 - \frac{N^0(f, N)}{N} \end{aligned}$$

Where:

- $N^1(f, N) = \sum_{k=1}^N |FDAF(k, f)|^2$ , the number of times the  $f$  component of the FDAF filters equals one,
- $N^0(f, N) = N - \sum_{k=1}^N |FDAF(k, f)|^2$ , the number of times the  $f$  component of the FDAF filters equals zero.

The FDAF filters  $FDAF_m(k, f, i)$  calculated in (6) assumed only one pulse pair from station  $i$  was received. In this case, the expectation of the FDAF filter equals:

$$\begin{aligned} E[FDAF(k, f)] &= \lim_{N \rightarrow +\infty} 1 - \frac{N_1^0(f, i)}{N} \\ &= 1 \quad \forall f \end{aligned}$$

Where:

- $N_1^0(f, i) = \sum_{k=1}^N FDAF_m(k, f, i)$ ,
- $FDAF_m(k, f, i)$  being the FDAF filters calculated in (6).

In real interference environments, pulses are emitted periodically. Knowing station  $i$  PRF, one can derive the number of pulse pairs emitted by station  $i$  during  $T$  seconds,  $N_{pulse}(i, T)$ :

$$N_{pulse}(i, T) = PRF(i) \times T$$

Where:

- $PRF(i)$  is the  $i^{\text{th}}$  station Pulse repetition frequency,
- $T = R \times N \times T_s$ , where  $T_s$  is the sampling period,  $R$  is the window width in samples and  $N$  is the number of observed windows.

Assuming that each pulse pair emitted by the same station arrives at a different time instant, and that each of them induces the same number of zeros in

the FDAF filters, the expectation of the FDAF filters becomes:

$$\begin{aligned} E\left[FDAF(k, f)\right]^2 &= \lim_{N \rightarrow +\infty} 1 - \frac{N^0(f, N)}{N} \\ &= \lim_{N \rightarrow +\infty} 1 - \frac{N_1^0(f, i) \times N_{pulse}(i, T)}{N} \\ &= \lim_{N \rightarrow +\infty} 1 - \frac{N_1^0(f, i) \times PRF(i) \times R \times N \times T_s}{N} \\ &= \lim_{N \rightarrow +\infty} 1 - N_1^0(f, i) \times N_{pulse}(i, T_{win}) \\ &= 1 - N_1^0(f, i) \times N_{pulse}(i, T_{win}) = \end{aligned}$$

Where:

- $N_1^0(f, i)$  is the number of times the  $f$  component of the FDAF filters equals zero, assuming only one pulse pair is received from station  $i$ ,
- $T_{win}$  is the duration of one window of R samples in seconds.

Several stations being visible, other pulse pairs will reach the receiver. In case two interferences are received simultaneously, the FDAF filters behaviour will differ from (6), and will depend on the carrier frequency, the phase and the power of the considered pulses. Assuming, in a first approximation that this can not occur, the total contribution is the sum of each station contribution:

$$E\left[FDAF(k, f)\right]^2 = 1 - \sum_{i=1}^M N_1^0(f, i) \times N_{pulse}(i, T_{win})$$

Then, the FDAF equivalent transfer function is:

$$\left|H_{eq, FDAF}(f)\right|^2 = 1 - \sum_{i=1}^M N_1^0(i) \times N_{pulse}(i, T_{win}) \quad (8)$$

The post correlation  $C/N_0$  degradation is then calculated using equation (7), and equations (2) and (3) where  $\left|H_{eq, FDAF}\right|^2$  is replaced by the result given in (8).

## COLLISION STRATEGY

The equivalent filter calculated above neglects the effect of pulses collisions. Basically, a collision occurs when two interferers are received at the same time. The effect can be an increase (constructive collision), or a decrease (destructive collision) of the received signal amplitude, and so of the interference detection rate.

In the presented tool, collisions have been taken into account by calculating the FDAF equivalent filters and the interference coefficient in case two interferences are received at the same instant. The

methodology used to calculate this equivalent filter is the same than the one used assuming no collisions occur. The FDAF equivalent transfer function taking collisions into account is thus:

$$H_{eq,FDAF,col}(f) = H_{eq,FDAF,no\_col}(f) \times P_{no\_col} + \sum_{i=1}^M \sum_{j=1}^M H_{eq,FDAF,col}(i,j)(f) \times P_{one\_col}(i,j)$$

Where:

- $P_{no\_col}$  is the probability that no collisions occur,
- $P_{one\_col}(i,j)$  is the probability that interferences from stations  $i$  and  $j$  arrived at the same instant,
- $H_{eq,FDAF,no\_col}(f)$  is the FDAF equivalent transfer function assuming no interference collision occurrence,
- $H_{eq,FDAF,col}(i,j)(f)$  is the FDAF equivalent transfer function assuming interferences from stations  $i$  and  $j$  arrived at the same instant.

The time separating the reception of two interferences is supposed to follow a Poisson law. Then, the probability that interference  $i$  and interference  $j$  collide has been determined as the probability that their inter-arrival time is smaller than  $6.8 \mu s$ .

$$P_{one\_col}(i,j) = (\lambda \times \tau)^2 \times e^{-\lambda \times \tau}$$

Where:

- $\lambda = PRF(i) + PRF(j)$  is the Poisson law parameter,
- $\tau = 6.8 \mu s$ .

The chosen duration ( $6.8 \mu s$ ) represents the equivalent time duration of one pulse.

## DEGRADATION MAPS

The described tool has been run over Europe, with a latitude and longitude step of  $1^\circ$ . The FDAF characteristics are  $R=128$  samples and the threshold has been fixed to  $-190.4$  dBW/Hz. Simulations showed this threshold was a good trade off between false alarm rate (interference detection due to noise only) and interference detection capability, resulting in optimal FDAF performance over the European hot spot. The Europe sky has been covered considering latitudes going from 35 to 72 degrees, from Spain to Norway, and longitudes going from  $-15$  to 45 degrees, from east Island to west Russia.

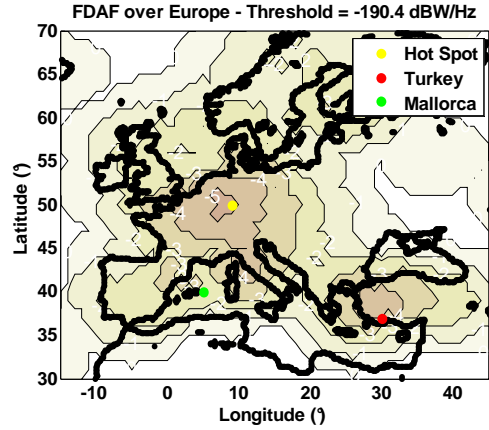


Figure 10:  $C/N_0$  degradation at correlator output, over Europe using FDAF against DME/TACAN signals.

Figure 10 shows the degradation values in dB over the described map. The results obtained seem coherent: the hot spot is easily visible (over Germany) and the degradation decreases when flying away from it. In addition, we can observe two other warm spots: one over turkey and another over Mallorca. When flying overseas, the degradation is almost zero, which is consistent with what could be expected.

These results can be compared to the ones presented in the map shown in Figure 11. These results represent the degradation assuming the use of the TB technique and have been obtained using the derivation method presented in [Bastide, 2004], and the same interference characteristics generator than for FDAF.

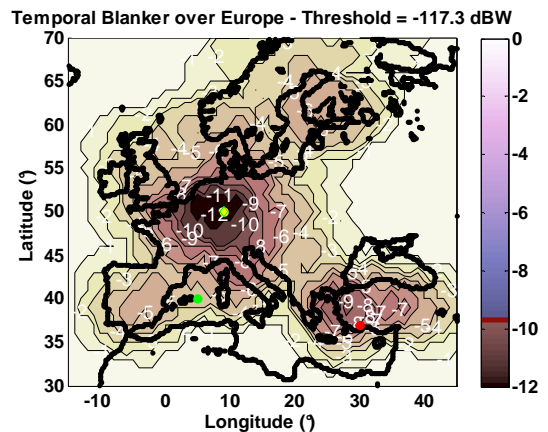


Figure 11:  $C/N_0$  degradation at correlator output, over Europe using TB against DME/TACAN signals.

The results provided in previous figures need to be validated, or at least corroborated. The following paragraph presents simulation results using FDAF or TB in a simulation GNSS receiver, over the three

spotted locations: the European hot spot, a place in Turkey and Mallorca.

## SIMULATOR DESCRIPTION

The performances of the techniques were obtained using a software simulator called PULSAR, depicted in [Bastide, 2004]. The simulator is developed under Labview and is composed of:

- A signal generation block. This block generates an E5a signal, thermal noise, and pulsed interferences.
- A signal processing block composed of a front end filter, an AGC/ADC, the two presented IMTs and correlators.
- Code and carrier phase tracking loops.

Then, a  $C/N_0$  estimator provides its value at correlation output. The carrier to noise density is calculated using the following formula [Betz, 2000]:

$$\frac{C}{N_0} = \frac{E[I_p]^2}{\text{Var}[I_p]} \times B_{PD}$$

Where:

- $I_p$  are the prompt Inphase samples,
- $B_{PD}$  is the PreDetection Bandwidth.

The number of inphase samples used in the mean and the variance estimators was set to 10. The predetection bandwidth is the inverse of the coherent integration time, which is the time required to output one correlator sample (10 ms in our case). Then, each carrier to noise density ratio estimate is passed through an averaging filter using 4 values.

## SIMULATION SIGNAL ENVIRONMENT

The simulations were run using signal environment assumptions made in the corresponding paragraph. More precisely, interference signals were generated assuming the GNSS receiver was located over the European hot spot, over Spain (Mallorca), and turkey. In the simulator, the interference environment is defined using the same generator than in the prediction tool. From a database composed of DME/TACAN beacon coordinates, emission powers, carrier frequencies and PRF, it calculates the link budget and outputs a file readable by the simulator gathering the required

information. Then, a Matlab routine generates the interfering signal combining the DME sources received by the receiver at arrival times determined using a Poisson law.

## SIMULATION RESULTS

Six scenarios were tested: the two techniques are tested over the three remarkable locations.

The Temporal Blanker threshold has been set to -117.3 dBW, which is considered as the threshold minimizing  $C/N_0$  degradations on E5a due to pulsed interference over the European hot spot [Bastide, 2004]. The FDAF window size has been set to 128 samples, and the threshold to -190.4 dBW/Hz, optimizing FDAF performance over the European hot spot.

The tool could be validated only if tested in different interference conditions: the frequency repartition of the interference had to vary from one place to another along with the density in interference. Thus, the chosen locations are [40,5] (Mallorca, Spain), [50,9] (hot spot, Germany) and [37,30] (Turkey). An indication of the interference source frequency repartition is given for each location in Figure 12, Figure 13 and Figure 14.

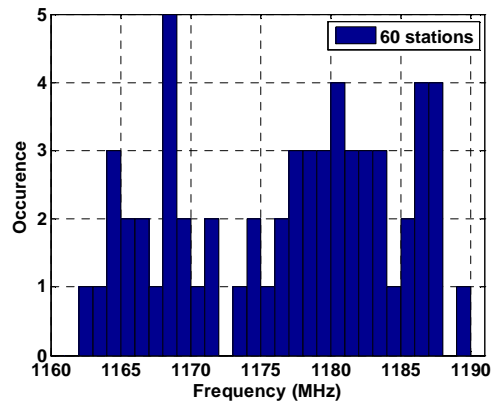


Figure 12: DME/TACAN carrier frequency repartition over European Hot Spot.

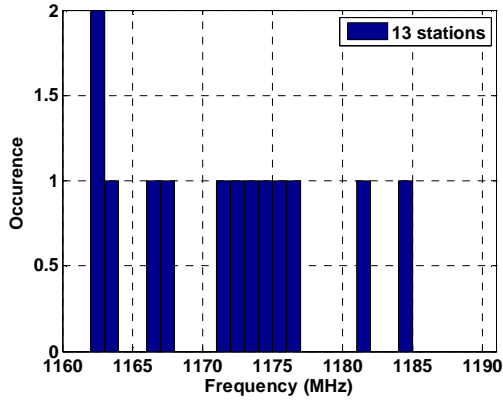


Figure 13: DME/TACAN carrier frequency repartition over Mallorca.

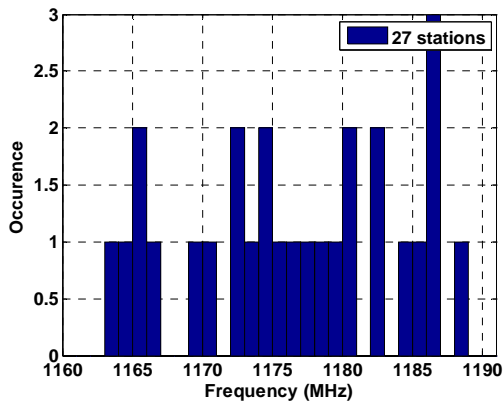


Figure 14: DME/TACAN carrier frequency repartition over Turkey.

The results obtained using the prediction tool are also given for comparison. Table 1 confronts the results obtained using the simulator and the map derivation tool.

Table 1:  $C/N_0$  degradations in dB.

	Degradations Results	
	Simulator	Map
IMT	Temporal Blanker	FDAF 128
Turkey	6.16 / 7.2	3.75 / 3.91
Mallorca	2.72 / 4.1	1.88 / 2.48
Hot Spot	11.6 / 11.69	5.07 / 5.56

The TB prediction tool is more pessimistic than the simulator, the maximum prediction error being of about 1 dB. The FDAF prediction tool results are closer to the simulator ones. The tool is validated for both techniques, with a precision of about 1.5 dB for TB and 0.5 dB for FDAF.

With the considered settings, FDAF shows better performance than the TB, whatever the over flight region, what was expected. The gain is of about 5 dBs over the hot spot, which may justify the implementation of the technique. It is possible to use even more samples in the Fourier Transform estimation (256, 512...) but the corresponding performance increase may not be significant enough.

It has to be noticed that the degradation estimated using the TB is different from the one obtained in [Bastide, 2004]. The simulator has been slightly modified:

- the front end filter was simplified. Shaper than the previous one, it induces greater correlation losses, but requires less computation load. It still complies with EUROCAE E5/L5 masks given in [Bastide, 2004].
- the uniform non centred quantization law has been changed in a centred uniform one,
- the sampling frequency has been set to 56 MHz.

The two last modifications were made so as to make a simulator as similar as possible to the GNSS receiver mock-up designed for the ANASTASIA project.

The aircraft antenna gain has also been modified, taking into account EUROCAE WG-62 new assumptions for low elevations. In [Bastide, 2004], the pattern used was extracted from [RTCA, 2004]. The values are -6 dBi at 0 degree decreasing linearly with angle to -10 dBi at -30 degrees, the interference reception angles lying in this elevation range. The EUROCAE WG-62 decided to test GNSS receivers using the maximum specified gain (0° dBi, see [EUROCAE WG-62, 2006]) for all elevations, inducing an increase of the impact of the interference on the receiver.

Moreover, the new degradation value of approximately 12 dBs over the hot spot using TB implies that this technique can not be used in onboard receivers as the unique IMT. The guaranteed minimum  $C/N_0$  is not sufficient to respect the  $C/N_0$  acquisition thresholds imposed by civil aviation authorities. In this case, the FDAF is the only technique that could allow a GNSS receiver to be certified to be used onboard an aircraft.

## CONCLUSION

In this paper, a methodology enabling FDAF performance prediction as a function of the interference environment without using heavy simulations has been depicted and validated.

The developed prediction tool has been tested over Europe, and the results were compared to TB

results obtained using a TB performance prediction described in [Bastide, 2004], using the same scenarios. Each technique has been set so as to show optimal performance, and FDAF definitely shows better performance than the TB. It has been seen that the latter technique is costless compared to FDAF, but considering the new EUROCAE assumptions about aircraft antenna gain, the 12 dB post-correlation  $C/N_0$  degradation suffered by such receivers prevents a GNSS receiver using the TB as only pulsed interference mitigation technique from standing this kind of heavy interference scenario, and hence does not comply with civil aviation requirements. In addition, [Bastide, 2004] showed that GNSS receivers can stand 8 dBs of  $C/N_0$  decrease due to pulsed interference, and stand ICAO requirements on acquisition time. The EUROCAE antenna gains assumptions definitely need to be deeper discussed.

## ACKNOWLEDGMENTS

This work has been funded by the ANASTASIA project. This project is financed through EC DG Research in the framework of FP6.

## REFERENCES

- [Bastide, 2004], Bastide F.: *Analysis of the Feasibility and Interests of Galileo E5a/E5b and GPS L5 Signals for Use with Civil Aviation*, PhD. Thesis, 2004.
- [Monnerat, 2003], Monnerat M., Erhard P., Lobert B.: *Performance Analysis of a GALILEO Receiver Regarding the Signal Structure, Multipath, and Interference Conditions*, ION GNSS 2003.
- [Grabowsky, 2002], Grabowsky J., Hegarty C.: *Characterization of L5 Receiver Performance Using Digital Pulse Blanking*, Proceeding of The Institute of Navigation GPS Meeting, Portland, OR, September 2002.
- [Van Dierendonck, 1996], Van Dierendonck A.J.: *"GPS receivers", Global Positioning System: Theory and Application*, B.Parkinson and J.J Spilker, JR., Ed ., Washington, D.C.: AIAA, Inc., 1996.
- [EUROCAE WG-62, 2006], Eurocae WG-62 works: *Interim Minimum Operational Performance Specification For airborne Galileo Satellite Receiving equipment (White Paper)*, May 2006.
- [Raimondi, 2006], Raimondi M., Macabiau C., Bastide F., Julien O.: *Mitigating Pulsed Interference Using Frequency Domain Adaptive Filtering*, ION GNSS 2006.
- [RTCA, 2004], RTCA SC-159: *Assessment of Radio Frequency Interference Relevant to the GNSS L5/E5a*, RTCA DO 292, July 2004.
- [Betz, 2000], Betz J.W.: *Effect of Narrowband Interference on GPS Code Tracking Accuracy*, *Proceedings of the Institute of Navigation Technical Meeting*, Anaheim, CA, January 2000.